BJ www.biochemj.org

BJ Signal

Biochem. J. (2012) **443**, 287–295 (Printed in Great Britain) doi:10.1042/BJ20120035

Mechanism and specificity of the human paracaspase MALT1

Janna HACHMANN*†, Scott J. SNIPAS*, Bram J. VAN RAAM*, Erik M. CANCINO‡, Emily J. HOULIHAN*, Marcin POREBA§, Paulina KASPERKIEWICZ§, Marcin DRAG§ and Guy S. SALVESEN*[1]

*Sanford-Burnham Medical Research Institute, La Jolla, CA 92037, U.S.A., †Graduate School of Biomedical Sciences, Sanford-Burnham Medical Research Institute, La Jolla, CA 92037, U.S.A., ‡University of California, San Diego, La Jolla, CA 92093, U.S.A., and §Wroclaw University of Technology, Wybrzeze Wyspianskiego 27, 50-370 Wroclaw, Poland

The paracaspase domain of MALT1 (mucosa-associated lymphoid tissue lymphoma translocation protein 1) is a component of a gene translocation fused to the N-terminal domains of the cellular inhibitor of apoptosis protein 2. The paracaspase itself, commonly known as MALT1, participates in the NF-κB (nuclear factor κB) pathway, probably by driving survival signals downstream of the B-cell antigen receptor through MALT1 proteolytic activity. We have developed methods for the expression and purification of recombinant full-length MALT1 and its constituent catalytic domain alone. Both are activated by dimerization without cleavage, with a similar dimerization barrier to the distantly related cousins, the apical caspases. By using positional-scanning peptidyl substrate libraries we demonstrate that the activity and specificity of full-length MALT1 is recapitulated by the catalytic domain alone, showing a stringent requirement for cleaving after arginine, and with striking peptide length constraints for efficient hydrolysis. Rates of cleavage (k_{cat}/K_m values) of optimal peptidyl substrates are in the same order (10^3–10^4 $M^{-1} \cdot s^{-1}$) as for a putative target protein CYLD. Thus MALT1 has many similarities to caspase 8, even cleaving the putative target protein CYLD with comparable efficiencies, but with diametrically opposite primary substrate specificity.

Key words: CYLD, mucosa-associated lymphoid tissue lymphoma translocation protein 1 (MALT1), paracaspase, positional-scanning substrate library, protease, substrate specificity.

INTRODUCTION

The human protein MALT1 (mucosa-associated lymphoid tissue lymphoma translocation protein 1) was discovered over a decade ago as a component of a genetic translocation. In this translocation, the *MALT1* gene is fused to the gene encoding cIAP2 [cellular IAP (inhibitor of apoptosis protein) 2] [1,2]. The protein product of this gene fusion contains the N-terminal domains of cIAP2 fused to the C-terminal region of MALT1. Although it was soon realized that MALT1 plays a part in the NF-κB (nuclear factor κB) pathway [2], the exact nature of its function remains under investigation.

It has been proposed that antigen receptor engagement leads to the phosphorylation of the adaptor protein CARMA1 [CARD (caspase recruitment domain)-containing MAGUK (membrane-associated guanylate kinase) 1] (also known as CARD11), followed by recruitment of MALT1 and its constitutive binding partner Bcl10 [3–6]. CARMA1, Bcl10 and MALT1 together form the CBM complex, which serves as a binding platform for several other proteins, among them TRAF6 [TNF (tumour-necrosis-factor)-receptor-associated factor] and NEMO (NF-κB essential modulator) also known as IKKγ [IκB (inhibitor of NF-κB) kinase] [7], which leads to the induction of NF-κB target genes.

Full-length MALT1 is made up of several domains. Downstream of a DD (death domain) and Ig-like domains, MALT1 contains a region which shows similarity to the caspase family of proteases [2] (Figure 1A). After initial unsuccessful attempts to demonstrate proteolytic activity [8], two groups independently reported proteolytic MALT1 substrates [9,10]. Rebeaud et al. [10] found MALT1 to cleave its binding partner Bcl10, whereas Coornaert et al. [9] reported cleavage of the negative NF-κB regulator A20. To date, three further substrates, NIK (NF-κB-inducing kinase), CYLD and RelB, have been found [11–13]. The results of substrate cleavage are diverse and include activation of canonical and non-canonical NF-κB as well as JNK (c-Jun N-terminal kinase) signalling [9,11–13] and increased T-cell-receptor-controlled binding to fibronectin [10].

All reported MALT1 substrates are cleaved directly C-terminal to an arginine residue in the P1 position (according to Schechter and Berger [14] nomenclature, P1 corresponds to the amino acid directly N-terminal to the cleavage site). Thus MALT1 has been proposed to be an arginine-specific protease. To test this proposal, and to define the substrate preference, catalytic properties and activation mechanism of MALT1, we have performed biochemical characterization studies of purified recombinant MALT1 expressed in *Escherichia coli*.

EXPERIMENTAL

Materials

All chemicals were purchased from commercial suppliers unless otherwise stated. See individual sections for details.

Protein expression and purification

Constructs encoding full-length MALT1-WT (wild-type) and -C464A were a gift from Dr Margot Thome (Department of Biochemistry, University of Lausanne, Lausanne, Switzerland). These were cloned into a modified pET29b vector (Novagen)

Abbreviations used: Ac, acetyl; ACC, 7-amino-4-carbamoylmethylcoumarin; AFC, 7-amino-4-trifluoromethylcoumarin; AMC, 7-amino-4-methylcoumarin; BIR, baculovirus inhibitor of apoptosis protein repeat; CARD, caspase recruitment domain; CARMA1, CARD-containing MAGUK (membrane-associated guanylate kinase) 1; cIAP2, cellular inhibitor of apoptosis protein 2; DD, death domain; DTT, dithiothreitol; FKBP, FK506-binding protein; FMK, fluoromethylketone; HEK, human embryonic kidney; IAP, inhibitor of apoptosis protein; IPTG, isopropyl β-D-thiogalactopyranoside; JNK, c-Jun N-terminal kinase; MALT1, mucosa-associated lymphoid tissue lymphoma translocation protein 1; NF-κB, nuclear factor κB; NIK, NF-κB-inducing kinase; Ni-NTA, Ni^{2+}-nitrilotriacetate; PS-SCL, positional-scanning substrate combinatorial library; TCA, trichloroacetic acid; WT, wild-type; z, benzyloxycarbonyl.

[1] To whom correspondence should be addressed (email gsalvesen@sanfordburnham.org).

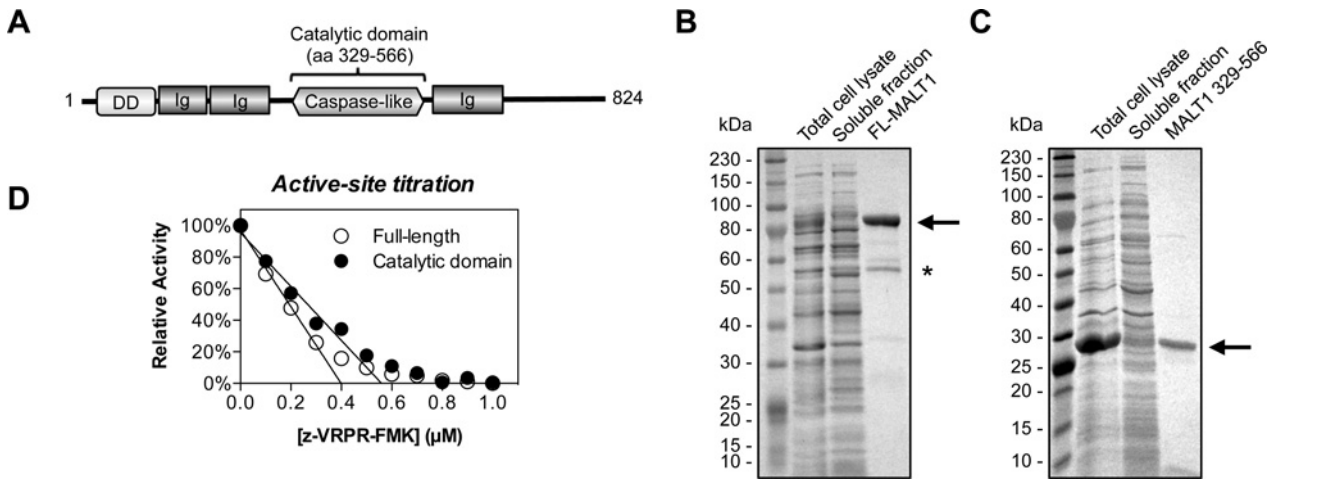

Figure 1 Domain structure and purification of MALT1

(**A**) Domain structure of MALT1. (**B** and **C**) His-tagged full-length MALT1 (**B**) and the catalytic domain (amino acids 329–566) (**C**) were expressed in *E. coli* and purified using a Ni-NTA column. Lane 1, molecular mass markers; lane 2, total cell lysate; lane 3, soluble material after sonication; lane 4, the eluted protein fraction with full-length (FL) MALT1 (**B**) and catalytic domain (**C**) respectively, depicted by arrows. The band marked with an asterisk (*) was N-terminally sequenced and found to be the *E. coli* heat-shock protein DnaK. (**D**) Full-length and catalytic domain MALT1 were titrated with the depicted concentration range of the irreversible inhibitor z-VRPR-FMK. The linear portion of the titration curve was extrapolated to its intercept of the *x*-axis to reveal the active concentration of the respective MALT1 preparations.

containing an N-terminal Strep II tag and a C-terminal His tag and transformed into BL21(DE3) *E. coli* cells. Protein expression was induced with 0.04 mM IPTG (isopropyl β-D-thiogalactopyranoside) and cultures were grown overnight at 18 °C. The soluble fraction was applied to a Ni-NTA (Ni^{2+}-nitrilotriacetate) column and eluted with 200 mM imidazole or, for increased purity, an imidazole gradient from 0 to 200 mM in 50 mM Hepes and 100 mM NaCl (pH 7.5). The catalytic domain (amino acids 329–566) [8] was cloned into pET21b (Novagen) containing a C-terminal His tag. It was expressed and purified as above except that 0.2 mM IPTG was used and cultures were grown at 25 °C for 4 h. The protein concentration was determined by absorbance at 280 nm on the basis of the estimated molar absorption coefficient [15]. Proteins were resolved by SDS/PAGE (8 % or 8–18 % gels) and stained with Gel Code Blue reagent (Thermo Scientific).

Synthesis and assay of the P2–P4 PS-SCL (positional-scanning substrate combinatorial library)

The ACC (7-amino-4-carbamoylmethylcoumarin)-coupled PS-SCL was synthesized on the basis of a concept described previously [16]. Arginine was fixed in the P1 position. After synthesis, each sub-library was dissolved at a concentration of 2.5 mM in biochemical-grade dried DMSO and stored at − 20 °C until use. Each sub-library contained 361 individual substrates and was measured at a total substrate concentration of 50 μM (individual substrates at a concentration of approximately 138.5 nM). Full-length and catalytic domain MALT1 (see Figures for enzyme concentrations) were pre-incubated at 37 °C in assay buffer [50 mM Hepes, 100 mM NaCl, 0.9 M sodium citrate and 10 mM DTT (dithiothreitol) (pH 7.5)] plus (for the catalytic domain) 1 mM EDTA for 20 min before addition to the library and measurement of substrate hydrolysis rates. Release of fluorophore was monitored continuously with excitation at 355 nm and emission at 460 nm with an assay time of 2 h. Rates were determined from the linear portion of the progress curves. The maximum value of each sub-library was set at 100 % and the other values were adjusted accordingly.

Synthesis and assay of the P1 library

All substrates for the screening of the P1 position with the sequence Ac-Leu-Arg-Ser-X-ACC, where Ac is acetyl and X represents either a natural amino acid or norleucine as a substitute for methionine, as well as other individual fluorigenic ACC-coupled substrates, were synthesized on a solid-state support (Rink resin) and purified using reverse-phase HPLC preparatory chromatography according to a protocol described previously [17]. Substrates were tested at a concentration of 10 μM in assay buffer plus 1 mM EDTA. Before addition of the substrate, enzyme was pre-incubated in buffer for 20 min at 37 °C. Catalytic rates were determined as described in the previous section.

Comparison of substrates

Cleavage of fluorigenic substrates of different lengths by full-length or catalytic domain MALT1 was tested in assay buffer plus 1 mM EDTA. Enzyme was pre-incubated in buffer for 20 min at 37 °C before addition of the substrate at a concentration of approximately 20 μM. To determine catalytic rates, different potential MALT1 substrates were assayed between 0 and 100 μM in assay buffer plus 1 mM EDTA. Before addition of substrate, MALT1 was pre-incubated at 37 °C in buffer as described above. AFC (7-amino-4-trifluoromethylcoumarin)- and AMC (7-amino-4-methylcoumarin)-coupled peptide substrates were obtained from SM Biochemicals. The active concentration of enzyme for the determination of catalytic rates was determined by titration with the irreversible inhibitor z-VRPR-FMK (Enzo Life Sciences) (where z is benzyloxycarbonyl, VRPR is Val-Arg-Pro-Arg and FMK is fluoromethylketone) [18].

Hofmeister series

MALT1 (full-length and catalytic domain) was assayed in 50 mM Hepes, 10 mM DTT and 1 mM EDTA (pH 7.5), with salt concentrations ranging from 0 to 1 M. Enzyme was pre-incubated for 20 min at 37 °C in the appropriate buffers before addition of Ac-LRSR-AFC at 100 μM and determination of the initial velocity.

Concentration-dependence of activity

Full-length MALT1 at a constant concentration of 500 nM was assayed in 50 mM Hepes, 100 mM NaCl, 10 mM DTT and 1 mM EDTA (pH 7.5) with citrate concentrations varying between 0.1 and 0.9 M. The reactions were supplemented with catalytic mutant at the concentrations indicated in Figure 1(D) and pre-incubated for 20 min at 37 °C before the addition of 100 μM Ac-LRSR-AFC.

Expression and purification of CYLD

A construct encoding recombinant human CYLD (isoform 2) was a gift from Dr Sumit Chanda (Sanford-Burnham Medical Research Institute, La Jolla, CA, U.S.A.). It was cloned with a C-terminal FLAG tag in pCDNA3.1 (Invitrogen) and expressed in and purified from HEK (human embyonic kidney)-293T cells as follows. Cells were grown to ~60 % confluence in 10 cm tissue culture dishes and transfected with 5 μg of plasmid DNA/dish using Nanojuice (Novagen/EMD Chemicals), according to the manufacturer's instructions. After transfection, cells were grown overnight, harvested, pooled, washed with PBS and lysed in 1 ml of cell lysis buffer [50 mM Hepes, 150 mM KCl, 0.1 % CHAPS and 1 % Nonidet P40 (pH 7.4)] supplemented with protease inhibitors [E-64, MG132, 3,4-DCI (3,4-dichloroisocoumarin), pepstatin, PMSF and aprotinin (all at 10 μM) and 100 μM EDTA] for 20 min on ice. The cleared lysate was collected after centrifugation and incubated overnight with 20 μl of washed M2 anti-FLAG beads. Protein was eluted from the beads after washing away the unbound material with 40 μl of 3×FLAG peptide at a concentration of 5 mg/ml in PBS for 20 min on ice.

Stability of MALT1 in sodium citrate buffer

Full-length MALT1-WT and -C464A were incubated at 1.5 μM in assay buffer plus 1 mM EDTA for various time periods followed by TCA (trichloroacetic acid) precipitation. Samples were resolved by SDS/PAGE (8–18 % gels) and stained with Gel Code Blue reagent. For N-terminal sequencing, proteins were resolved by SDS/PAGE, followed by Western blotting on to PVDF membrane. The membrane was stained with Coomassie Brilliant Blue, and the appropriate bands were subjected to Edman degradation using an ABI Procise 492.

In vitro cleavage of protein substrates

CYLD-WT was diluted to a 1 μM final concentration and incubated with various concentrations of active full-length MALT1 or ΔDED-caspase 8 (purified as described previously [18]) respectively for 1 h at 37 °C in 20 mM Pipes, 100 mM NaCl, 0.8 M sodium citrate and 10 mM DTT (pH 7.2). The reaction was stopped by TCA precipitation. Cleavage was subsequently assessed by SDS/PAGE (8–18 % gels), followed by Western blotting with an anti-CYLD antibody [rabbit anti-CYLD, pAb (polyclonal antibody) AF888 from Enzo Life Sciences] or with an anti-FLAG antibody (clone M2, Sigma–Aldrich). Blots were scanned on an Odyssey infrared scanner (LI-COR Biosciences) and the fluorescent signal of full-length protein and the cleaved product was used to determine $E_{1/2}$, representing the concentration of protease that cleaves 50 % of the full-length substrate in time (t). The apparent value for k_{cat}/K_m was then determined with the half-life equation [18]:

$$\frac{k_{cat}}{K_m} = \frac{\ln 2}{t E_{\frac{1}{2}}}$$

RESULTS

Expression and purification of MALT1

To characterize the substrate specificity and the catalytic properties of MALT1, we expressed His-tagged versions of both the catalytic domain alone (amino acids 329–566) and the full-length protein in *E. coli* (Figures 1B and 1C). On the basis of the protein concentration estimated from the absorbance at 280 nm, active-site titration with the irreversible MALT1 inhibitor z-VRPR-FMK [10] revealed that the preparations of the catalytic domain alone contained only an estimated 5–10 % of active protein depending on the protein preparation, whereas the full-length protein was found to be fully active (Figure 1D). The reason for this could not be determined, but may be due to partly aggregated or denatured protein, implying that the catalytic domain alone is not as stable as the full-length protein. Mutation of the putative catalytic Cys^{464} to alanine (full-length numbering) abrogated catalytic activity for both versions on all of the substrates tested (results not shown).

In vitro activation of MALT1 by sodium citrate

In regular low-salt buffers or buffers with ionic concentrations in the physiological range, neither full-length nor catalytic domain MALT1 showed any proteolytic activity in our hands. Kosmotropic salts have been shown to increase the activity of many enzymes [19–22], the extent of which depends on the active state of the enzyme in question. To explore this aspect, we determined the ability of a number of different salts to generate activity in full-length and catalytic domain MALT1 (Figures 2A and 2B). High concentrations of sodium citrate or sodium sulfate dramatically enhanced the catalytic activity of both full-length and catalytic domain MALT1, more than 1000-fold, and lithium sulfate showed a minor activation. In contrast, NaCl and LiCl showed no activating potential. These results are fully consistent with the Hofmeister effect. It is not entirely clear how kosmotropic salts of the Hofmeister series activate enzymes, but it is believed that they decrease the entropy in the system, thereby allowing ordering and oligomerization processes to take place that are normally entropically unfavourable [23]. On the basis of these results, sodium citrate was determined as the activator of choice. In line with the prediction that MALT1 is a cysteine protease, activity was enhanced by DTT, which probably serves to reverse oxidation of the catalytic cysteine residue that occurs during purification. $CaCl_2$, EDTA and 1,10-phenanthroline had no substantial effect on the activity of MALT1, demonstrating that it is probably not a metal-dependent enzyme (Figure 2C and results not shown).

Activation mechanism

Kosmotrope-mediated ordering of active-site loops can increase the activity of a protease severalfold. In addition, enzymes that are activated by oligomerization can show much higher increases in activity [20]. MALT1 showed no activity in the absence of kosmotropes and a robust increase in the presence of sodium citrate, and we postulated that this represents activation by oligomerization.

To elucidate this further, we studied the effect of the protein concentration on the activation of MALT1, hypothesizing that an oligomerization process would decrease the requirement for sodium citrate activation. We assayed a constant concentration of MALT1-WT in buffers with increasing sodium citrate concentrations (Figure 2D). We then added increasing amounts of MALT1-C464A to this constant amount of MALT1-WT to

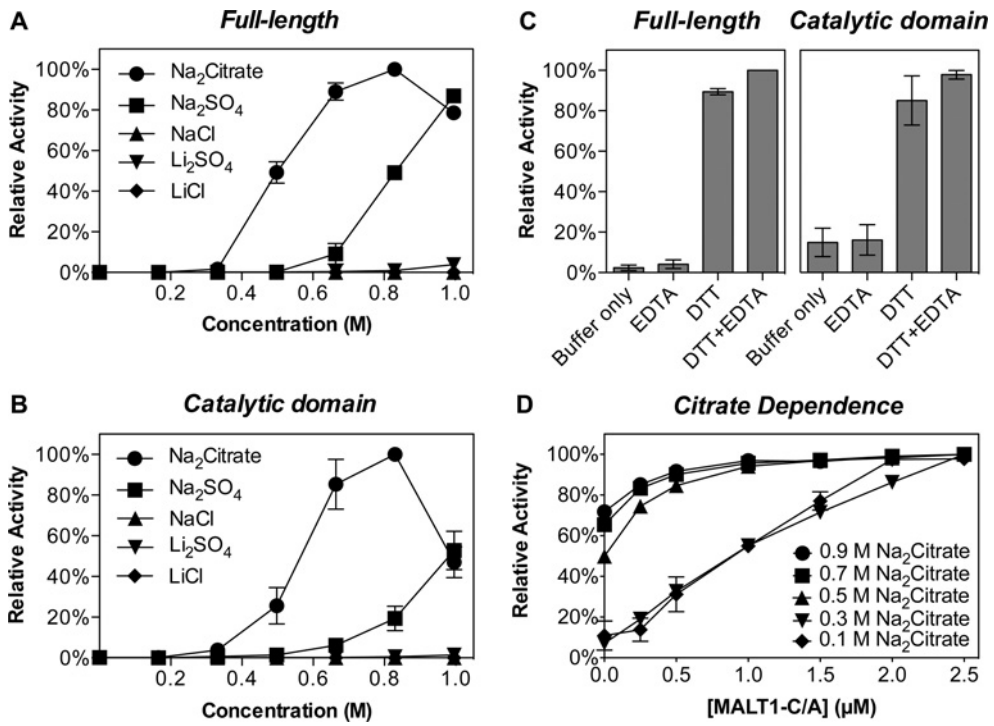

Figure 2 MALT1 activation

(**A**–**C**) Different salts and buffer additives were screened for MALT1-activating potential. Full-length (150 nM) and catalytic domain (4 μM) MALT1 were assayed in 50 mM Hepes (pH 7.5), 10 mM DTT and 1 mM EDTA, supplemented as depicted (**A** and **B**) or in 50 mM Hepes, 100 mM NaCl and 0.9 M sodium citrate (pH 7.5) supplemented as depicted (**C**). (**D**) Full-length MALT1-WT (500 nM) was assayed in buffers with various citrate concentrations and supplemented with full-length catalytic mutant as depicted. The experiments were repeated three (**A**–**C**) or two (**D**) times respectively. Mean values and S.E.M. are shown.

determine whether high concentrations of MALT1 decrease the influence of citrate on MALT1 activity. We found that at high sodium citrate concentrations, increasing the amount of enzyme only had a mildly activating effect. However, at low sodium citrate concentrations, increasing the amount of enzyme by adding MALT1-C464A led to a linear increase in MALT1 activity. We therefore speculate that MALT1 exists as a mixture of monomeric and oligomeric species. Sodium citrate addition and increased protein concentrations both shift this equilibrium towards the oligomeric (active) state. An unrelated control protein (catalytically inactive SENP1) had no effect on MALT1 (results not shown).

However, it is important to note that even the addition of very high concentrations of catalytic mutant to MALT1-WT at low citrate concentrations did not yield nearly as much activity as MALT1-WT at high citrate concentrations, either with or without the catalytic mutant. We conclude from this that sodium citrate acts in multiple ways, driving both the oligomerization processes and overall protein stabilization. The more the equilibrium favours oligomerization, as a consequence of a high enzyme concentration, the smaller the requirement for citrate becomes.

We sought to investigate the active conformation of MALT1 further by size-exclusion chromatography experiments of activated MALT1, but were unsuccessful because the activity of MALT1 was found not to be stable upon citrate depletion and high salt concentrations compromised the chromatography (results not shown).

MALT1 is active in the full-length unprocessed form

To further determine the mechanism of activation and the active conformation of MALT1, we tested whether the observed activation through sodium citrate leads to autoprocessing of MALT1. As visualized via SDS/PAGE in Figure 3, MALT1 remains largely unprocessed even after 2 h in sodium citrate, which leads to its activation. Several bands are visible in addition to full-length MALT1, but all are seen both in the WT and catalytic mutant, which rules out that they are autoprocessing products of

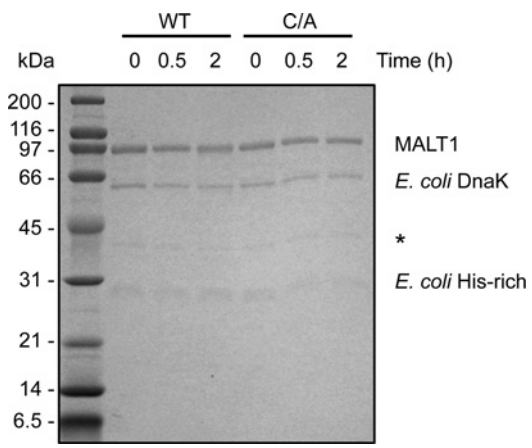

Figure 3 Sodium citrate does not activate MALT1 via cleavage

Full-length MALT1-WT and -C464A (C/A) were activated in assay buffer plus EDTA for the indicated times at 37°C. Reactions were stopped by TCA precipitation and samples were resolved by SDS/PAGE. The identity of all bands was determined via N-terminal sequencing. His-rich, FKBP-type peptidylprolyl *cis–trans* isomerase slyD (histidine-rich binding protein). The asterisk marks a protein that could not be clearly identified due to its low intensity, but partial sequencing showed that it did not match the sequence of MALT1. The molecular mass in kDa is indicated on the left-hand side.

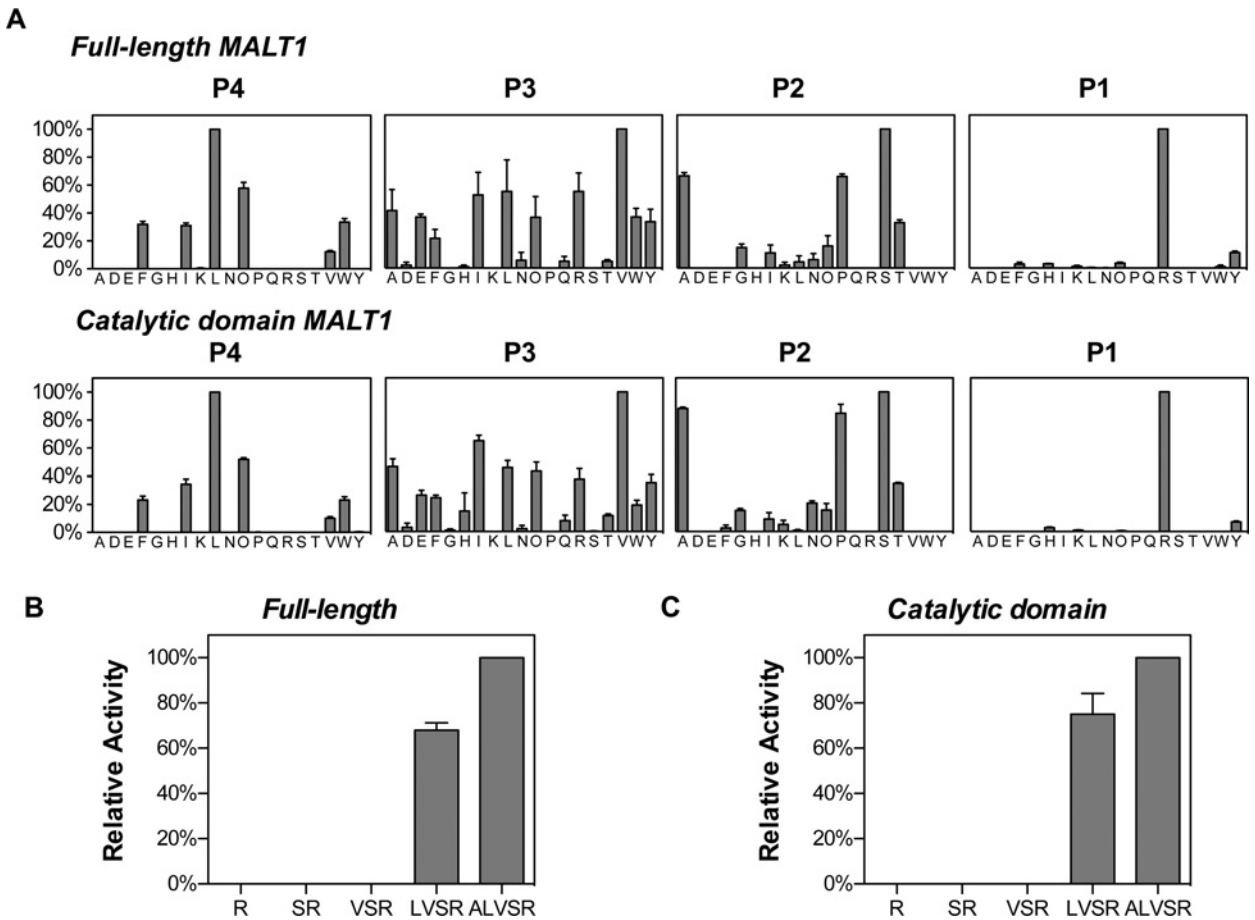

Figure 4 MALT1 substrate specificity

(**A**) MALT1 specificity was determined using a tetrapeptide P1 library consisting of Ac-LRSX-ACC (P1) and a P1-Arg PS-SCL (P2, P3 and P4). Full-length (130 nM) and catalytic domain MALT1 (5 μM) were analysed in assay buffer. Hydrolysis rates were determined and presented as a fraction of the maximal rate in each subset library position. The *x*-axes represent the amino acids depicted using the one-letter code (O, norleucine). (**B** and **C**) Cleavage of fluorigenic peptides of various lengths by full-length (**B**, 80 nM) or catalytic domain (**C**, 4 μM) was determined in assay buffer plus EDTA. The highest activity in each assay was set as 100 %; all other activities are shown relative to this. All assays were repeated at least three times. Mean values and S.E.M. are shown.

MALT1. We investigated their identity via N-terminal sequencing and found them to be *E. coli* impurities, rather than MALT1 autocleavage products. We therefore conclude that MALT1 is active in its full-length unprocessed form *in vitro* and does not process itself upon sodium citrate treatment in significant amounts.

Substrate specificity

Specificity of proteases is conventionally determined using fluorigenic or chromogenic reporter-coupled peptides as substrates that occupy the catalytic cleft of the enzyme. Thus, to determine the inherent substrate specificity of both full-length MALT1 and the catalytic domain, we screened a PS-SCL consisting of fluorigenic tetrapeptides.

MALT1 is commonly referred to as an arginine-specific protease. To further determine its substrate specificity, MALT1 was tested on a peptide library with the P1 position fixed to arginine and the P2, P3 and P4 positions varied to represent all possible combinations of proteinogenic amino acids (cysteine was omitted and norleucine was substituted for methionine). The full-length and the catalytic domain showed comparable substrate specificity (Figure 4A). The P2 position was moderately selective for amino acids with small side chains, with the small polar serine residue as well as non-polar hydrophobic amino acids such as proline and alanine residues well tolerated. MALT1 exhibited the greatest tolerance in the P3 position. The preferred amino acid in this position was valine, but it was closely followed by other non-polar hydrophobic amino acids and even polar charged residues were reasonably well tolerated. However, within this library it was the P4 position that showed the highest level of selectivity, with leucine clearly favoured. The closely related norleucine residue as well as isoleucuine were also tolerated, whereas polar residues in the P4 position completely abrogated protease activity.

After determining the P2, P3 and P4 specificities, we went on to test the selectivity for arginine in the P1 position using a P1 library. To decrease the number of non-cleavable substrates in the mixture and therefore increase the sensitivity of the approach, the P2, P3 and P4 positions were fixed to residues found favourable in the previous library screen. However, the optimal sequence LVSX contains two hydrophobic residues. In combination with an additional hydrophobic amino acid in the P1 position this can lead to solubility issues. We therefore synthesized a P1 library consisting of the less hydrophobic, yet still well tolerated, sequence Ac-LRSX-ACC (X representing all amino acids except cysteine; norleucine was substituted for methionine). Using this approach, high selectivity for arginine in the P1 position could be confirmed (Figure 4A, right-hand panels). Additionally, a minor yet consistent activity on tyrosine and to a lesser extent histidine in P1 was observed.

Table 1 Catalytic efficiencies of MALT1

Comparative catalytic efficiencies of full-length and catalytic domain MALT1. Values for the enzyme concentration were obtained using active-site-titrated enzymes, as described in the Experimental section. Standard errors are derived from non-linear regression analysis of the general Michaelis–Menten equation compared with the experimental data points. ALVSR, Ala-Leu-Val-Ser-Arg; LRSR, Leu-Arg-Ser-Arg; LVSR, Leu-Val-Ser-Arg.

Substrate	[Enzyme] (nM)	k_{cat} (s^{-1})	K_m (μM)	k_{cat}/K_m ($M^{-1} \cdot s^{-1}$)
Full-length-MALT1				
Ac-LVSR-ACC	399	0.071 (±0.0018)	15.3 (±1.1)	4.6×10^3
Ac-ALVSR-ACC	399	0.059 (±0.0025)	7.1 (±0.9)	8.4×10^3
Ac-LRSR-ACC	399	0.021 (±0.0014)	15.6 (±2.4)	1.3×10^3
Ac-LRSR-AMC	399	0.049 (±0.0024)	34.5 (±3.9)	1.4×10^3
Ac-LRSR-AFC	399	0.092 (±0.0036)	37.4 (±3.2)	2.5×10^3
Catalytic domain				
Ac-LVSR-ACC	285	0.095 (±0.0043)	8.9 (±1.3)	1.1×10^4
Ac-ALVSR-ACC	285	0.093 (±0.0036)	3.0 (±0.4)	3.1×10^4
Ac-LRSR-ACC	285	0.044 (±0.0011)	12.6 (±0.8)	3.5×10^3
Ac-LRSR-AMC	294	0.057 (±0.0033)	19.5 (±3.1)	2.9×10^3
Ac-LRSR-AFC	294	0.070 (±0.0036)	15.3 (±2.2)	4.6×10^3

It is important to note that the presence of EDTA did not influence the substrate specificity of MALT1. The PS-SCL was tested both in the absence and presence of EDTA and no substantial differences were observed. To underline this, the results are shown in the absence of EDTA for the full-length and in the presence of EDTA for the catalytic domain (Figure 4A). The optimal P4–P1 substrate preference of MALT1 was determined to be Leu-Val-Ser-Arg.

MALT1 has a minimum substrate length requirement for substrate hydrolysis

After determining the substrate specificity, peptides of various lengths were synthesized to verify both the PS-SCL results and determine the significance of the sequence length. Interestingly, a length of at least four residues was absolutely required (Figures 4B and 4C). No cleavage was observed if shorter peptides were used, even at a substrate concentration up to 20 μM. A pentapeptide composed of the four optimal residues determined in the library and alanine as an additional amino acid in the P5 position was designed. This elongation slightly increased the ability of the protease to cleave efficiently, but no stark increase, as for the switch from tripeptide to tetrapeptide, was observed.

The direct comparison of MALT1 activity on the Leu-Arg-Ser-Arg peptide, as often used in the literature as well as throughout the present study, with the Leu-Val-Ser-Arg peptide found as optimal in the library screen, showed the latter to have a 3–4-fold higher k_{cat}/K_m (Table 1), confirming data published by Hailfinger et al. [11]. This rather small difference again underlines the relatively flexible substrate preference of MALT1 in the P3 position. Increasing the substrate length from tetra- to penta-peptide further increased the catalytic efficiency 2–3-fold (Table 1). Owing to the inherent design of the PS-SCL, it was not possible to screen for preferences in P′ positions (C-terminal to the scissile bond). To determine whether changes in the fluorophore could alter the cleavage efficiency, Ac-Leu-Arg-Ser-Arg coupled to AMC, AFC and ACC was assayed. ACC contains a bulkier side chain than AMC and AFC, but no substantial differences were seen between the k_{cat}/K_m ratios of these three substrates (Table 1).

Cleavage of protein substrates

MALT1 and caspase 8 were both recently reported to cleave the deubiquitinating enzyme CYLD. MALT1 cleaves after Arg^{324} (isoform 1 numbering), activating JNK signalling [13], whereas caspase 8 was reported to cleave after Asp^{215}, abrogating necroptosis [24]. To compare catalytic efficiencies, we purified recombinant CYLD from HEK-293 cells and incubated it with increasing amounts of recombinant full-length MALT1 or the catalytic domain of caspase 8 under identical conditions, followed by analysis by SDS/PAGE (Figure 5). We found CYLD to be cleaved slightly more efficiently by MALT1 (k_{cat}/K_m, 1.4×10^3 $M^{-1} \cdot s^{-1}$) than by caspase 8 (k_{cat}/K_m, 1.2×10^3 $M^{-1} \cdot s^{-1}$).

DISCUSSION

Activation mechanism

MALT1 has been reported to be activated *in vivo* downstream of several immune activation receptors in a protein assembly known as the CBM complex [3–6]. Mechanistically, there are three distinct ways that a protease such as MALT1 can become active: proteolytic cleavage, conformational rearrangement of a monomer or conformational changes brought about by dimerization. We demonstrate that cleavage of MALT1 is not necessary for its activation. During the preparation of this paper, the crystal structure of the catalytic domain of MALT1, together with the C-terminally adjoining Ig-like domain, was published, revealing a dimeric arrangement mediated by the catalytic domain [25]. Our exploration of the activation mechanism using purified full-length and catalytic domain MALT1 adds direct experimental support to the idea that activation of proteolytic activity occurs through dimerization.

As well as the now identified structure of MALT1 itself, it is interesting to compare structures of MALT1 homologues and their mechanisms of activation for further insight into the mechanism of activation. MALT1 is a member of the peptidase clan CD, which includes caspases and caspase homologues [26]. Members of the caspase family can be activated via two main routes, but all caspases are active as dimers. The apical caspases 8, 9 and 10 are activated through dimerization, followed by a stabilizing, yet dispensable, cleavage reaction [20]. On the other hand, the executioner caspases 3 and 7 are obligate dimers that require cleavage for activation [27,28].

Another clan CD member worth considering is the arginine-specific protease R-gingipain. The crystal structure showed that in its active conformation the caspase-like domain of R-gingipain is subdivided into a catalytic domain and a stabilizing cap domain.

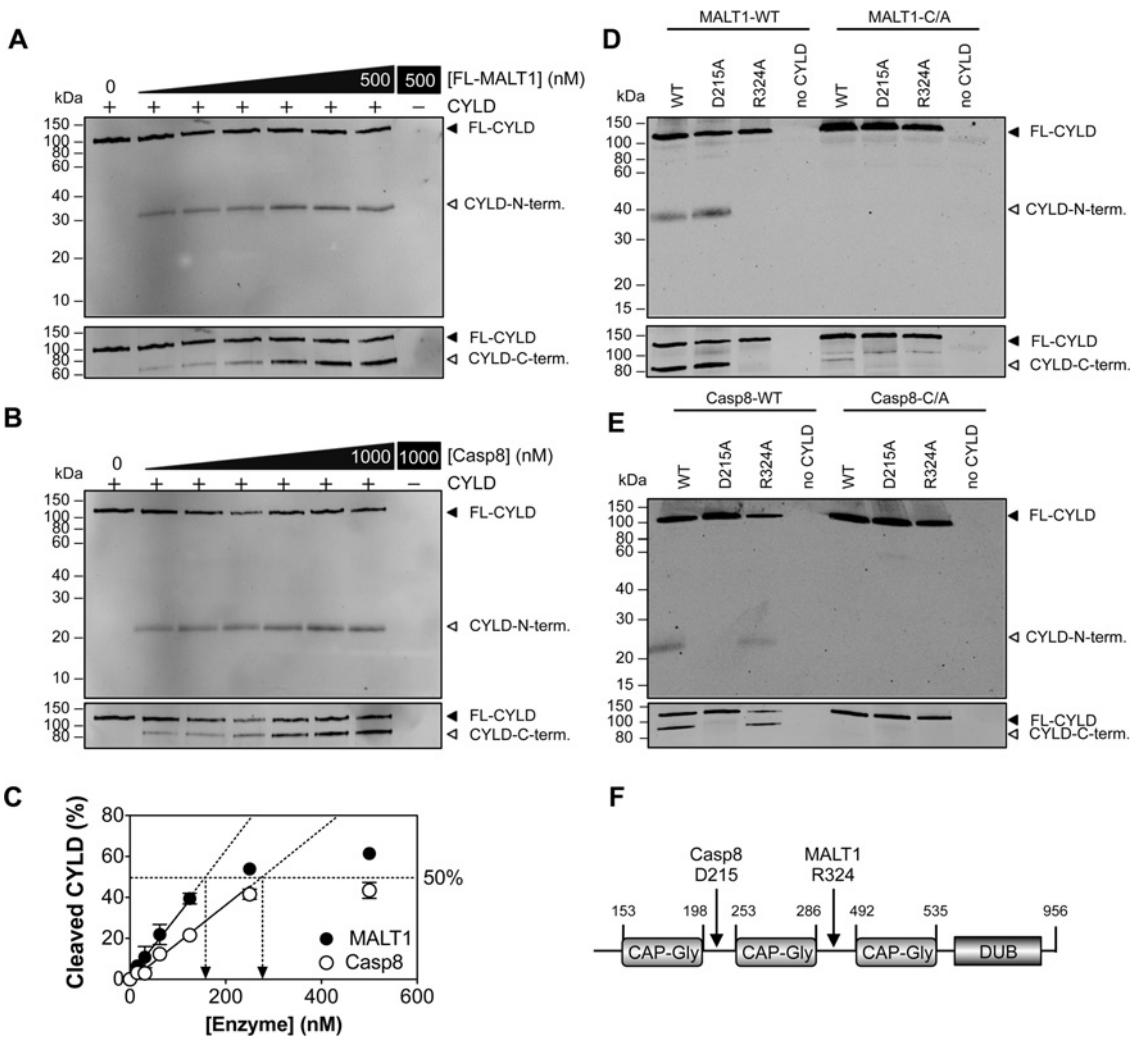

Figure 5 Cleavage of CYLD by MALT1 and caspase 8

(**A** and **B**) FLAG-tagged human CYLD was purified from HEK-293 cells and incubated with 2-fold increasing concentrations of full-length MALT1-WT (**A**) or caspase 8-WT (**B**) respectively. Samples were resolved by SDS/PAGE, followed by Western blotting and detection with an antibody against the N-terminal domain of CYLD (top panels) and anti-FLAG antibody (bottom panels) respectively. Data are representative of three independent experiments. (**C**) Linear regression used to determine the k_{cat}/K_m values. Mean values and S.D. are shown. (**D** and **E**) Different FLAG-tagged CYLD mutants were purified as in (**A**) and incubated with the WT or catalytic mutant versions of full-length MALT1 (**D**) or caspase 8 (**E**) respectively at 1 μM. (**F**) Overview of CYLD domains and cleavage sites. CAP-Gly, cytoskeleton-associated protein glycine-rich domain; DUB, deubiquitinating enzyme domain.

Both domains interact with an Ig-like domain, which further stabilizes the protein [29,30]. This is an interesting similarity to the structure of the catalytic domain of MALT1, which was crystallized together with an adjacent Ig-like domain. However, the Ig-like domains of R-gingipain and MALT1 interact with their respective protease domains, at least in the crystal structures, using different surfaces. In contrast with MALT1 and the caspases, R-gingipain, after several processing steps, is active as a monomer and does not require kosmotropic salts for activation. Thus MALT1 resembles apical caspases in its activation through dimerization.

The domain structure of MALT1 reveals an N-terminal DD, followed by two Ig-like domains, a caspase-like domain and another Ig-like domain (Figure 1A). Next to the catalytic domain, the crystal structures of the DD, as well as two Ig-like domains, were recently published [31]. The N-terminal Ig-like domains of MALT1 (amino acids 129–326) were found to behave as a tetrameric species involving a total of eight Ig-like domains, conceivably mimicking a multimeric activation platform. Other studies also support a multimeric platform for MALT1 activation. The oncogenic fusion protein where the DD (and sometimes the N-terminal Ig-like domains) of MALT1 are replaced by the three BIR (baculovirus IAP repeat) domains of cIAP2 was shown to constitutively activate the NF-κB pathway and promote cleavage of target proteins [2,9,12,13]. This is proposed to occur though dimerization, which could be mediated either through homotypic interactions between the BIR1 domains [32] or heterotypic interactions involving both the BIR domains and the C-terminal portion of MALT1 [33]. MALT1 dimerization hybrids with a gyrase B or helix–loop–helix domain, as well as multiple FKBP (FK506-binding protein) domains were shown to exhibit activity and NF-κB activation in cell transfection experiments [6,9,34]. Thus activation by dimerization resembles the mode of apical caspases, whose respective oligomerization assemblies provide platforms for the transition of latent monomers to active dimers [35]. Importantly, although the accessory domains of MALT1 are probably required for activation *in vivo*, our experiments demonstrate that the caspase-homology protease domain alone (devoid of Ig-like domains) is fully capable of providing maximal catalytic activity *in vitro*. We have not yet

been able to determine the dimerization equilibrium constant for MALT1, but it would seem to have a similar barrier for dimerization as the apical caspases, because MALT1 requires similar kosmotrope concentrations for optimal activation as caspases 8 and 10 [19].

Substrate specificity

Using PS-SCL we were able to determine the optimal cleavage sequence for MALT1. Both full-length and catalytic domain MALT1 prefer the P4–P1 sequence Leu-Val-Ser-Arg↓, with arginine being a near absolute requirement in the P1 position and leucine being strongly favoured in P4. The sequence determined matches the cleavage site in the reported natural substrate RelB perfectly [11]. The cleavage site of Bcl10 (Leu-Arg-Ser-Arg↓) is also very well matched [10]. However, looking at the other reported natural substrates, the fairly strict requirement for a leucine residue in P4 might seem surprising. Of the five protein substrates reported so far, only two show leucine in this position, whereas CYLD is cleaved after Phe-Met-Ser-Arg↓, NIK after Cys-Leu-Ser-Arg↓ and, remarkably, A20 after Gly-Ala-Ser-Arg↓ (a glycine residue in P4), which, according to the library screening results, is poorly tolerated. Notably, A20 contains leucine in the P5 position, which is favoured for cleavage by MALT1 (J. Staal, personal communication). Interestingly, MALT1 contains a large hydrophobic patch that forms the S4 pocket [25] that could, in principle, also accommodate a hydrophobic P5 residue to overcome the penalty of glycine in P4. In accordance with the broad P2 and P3 preferences obtained from our library data, the crystal structure demonstrates that these residues form fewer contacts with the S2 and S3 pockets [25], although the crystal structure would not appear to explain the preference for small side chains at P2.

The fairly strict preference in the P4 position is interesting considering that MALT1 is a caspase homologue. In caspases, the P4 position often plays a dominant role in promoting substrate specificity differences between paralogues [36]. Importantly, a length of at least four amino acids is required for cleavage to occur, another similarity to the caspases, which require substrates elongated beyond tripeptides for efficient cleavage [37].

Optimal peptide substrates were cleaved with rates (k_{cat}/K_m) of up to 10^4 $M^{-1} \cdot s^{-1}$, which is two to three orders of magnitude lower than for optimal caspase or gingipain substrates [30,38]. The low catalytic rates combined with the rather strict requirement for leucine in P4 explain why initial library screens conducted in our group several years ago did not reveal any proteolytic activity [8]. Thus MALT1 has a generally lower catalytic activity than other members of the clan to which it belongs, or additional factors are required to enhance activity of the recombinant material. It is important to keep in mind that, for the cleavage of natural protein substrates as opposed to peptide substrates, exosite interactions between protease and substrate often enhance cleavage of proteins that have non-optimal residues occupying the catalytic cleft [39]. From this perspective it is illuminating to consider the rate of cleavage of the natural substrate CYLD. k_{cat}/K_m was estimated at 1.4×10^3 $M^{-1} \cdot s^{-1}$, rendering this a slightly less efficient cleavage than the optimal peptide substrates. This raises the question as to whether MALT1 is simply not a very efficient protease on its natural substrates or peptide reporter substrates *in vitro*, or whether its truly optimal natural substrate has not yet been discovered. Even though some of the substrates determined to date show cleavage site sequences that are remarkably close to or identical with the sequence determined as optimal during the screening of the PS-SCL, it is important to keep in mind that MALT1 may enhance catalysis *in vivo* by an exosite-driven mechanism translating it from an enzyme of average efficiency to a highly effective protease given its ideal substrate.

Finally, we are struck by the similar rates of processing of CYLD by both MALT1 and caspase 8, representing a survival function for this apical caspase [24]. Since both of these events are reported to occur downstream of T-cell-receptor signalling [13,24] one would expect the distinct cleavages (see Figure 5F) to occur simultaneously since they have similar cleavage kinetics. If this is the case, the consequences of the MALT1 cleavage, leading to JNK activation [13], would be dominant since the fate of caspase 8-cleaved CYLD is degradation [24]. Naturally, the kinetics will depend on the rate of activation of the two proteases, and the rate of encounter within subcellular activation complexes.

AUTHOR CONTRIBUTION

Janna Hachmann, Scott Snipas, Bram van Raam, Erik Cancino and Emily Houlihan designed and performed the experiments. Marcin Drag designed, and Marcin Poreba and Paulina Kasperkiewicz synthesized the PS-SCLs and the synthetic substrates. Janna Hachmann and Guy Salvesen conceived the study and wrote the paper.

ACKNOWLEDGEMENTS

We thank Dr Jens Staal (Department of Biochemistry, Ghent University, Ghent, Belgium) for providing data before publication, Dr Margot Thome (Department of Biochemistry, University of Lausanne, Lausanne, Switzerland) for the gift of the full-length MALT1 plasmids, Dr Sumit Chanda (Sanford-Burnham Medical Research Institute, La Jolla, CA, U.S.A.) for providing the CYLD plasmid and Dr Peter D. Mace (Sanford-Burnham Medical Research Institute, La Jolla, CA, U.S.A) for critical reading of the paper before submission.

FUNDING

This work was supported by Genentech (grant-in-aid to J.H.), the Netherlands Organization for Scientific Research (NOW) (Rubicon fellowship to B.J.v.R.), the Barth Syndrome Foundation (to B.J.v.R.), the National Institutes of Health [grant number P30CA023100-27 (CURE supplement to Cancer Center Support Grant) (to E.M.C.)], and the Polish Foundation of Science (to M.D.).

REFERENCES

1 Dierlamm, J., Baens, M., Wlodarska, I., Stefanova-Ouzounova, M., Hernandez, J. M., Hossfeld, D. K., De Wolf-Peeters, C., Hagemeijer, A., Van den Berghe, H. and Marynen, P. (1999) The apoptosis inhibitor gene API2 and a novel 18q gene, MLT, are recurrently rearranged in the t(11;18)(q21;q21) associated with mucosa-associated lymphoid tissue lymphomas. Blood **93**, 3601–3609

2 Uren, A. G., O'Rourke, K., Aravind, L. A., Pisabarro, M. T., Seshagiri, S., Koonin, E. V. and Dixit, V. M. (2000) Identification of paracaspases and metacaspases: two ancient families of caspase-like proteins, one of which plays a key role in MALT lymphoma. Mol. Cell **6**, 961–967

3 Gaide, O., Favier, B., Legler, D. F., Bonnet, D., Brissoni, B., Valitutti, S., Bron, C., Tschopp, J. and Thome, M. (2002) CARMA1 is a critical lipid raft-associated regulator of TCR-induced NF-κB activation. Nat. Immunol. **3**, 836–843

4 Pomerantz, J. L., Denny, E. M. and Baltimore, D. (2002) CARD11 mediates factor-specific activation of NF-κB by the T cell receptor complex. EMBO J. **21**, 5184–5194

5 Wang, D., You, Y., Case, S. M., McAllister-Lucas, L. M., Wang, L., DiStefano, P. S., Nunez, G., Bertin, J. and Lin, X. (2002) A requirement for CARMA1 in TCR-induced NF-κB activation. Nat. Immunol. **3**, 830–835

6 Lucas, P. C., Yonezumi, M., Inohara, N., McAllister-Lucas, L. M., Abazeed, M. E., Chen, F. F., Yamaoka, S., Seto, M. and Nunez, G. (2001) Bcl10 and MALT1, independent targets of chromosomal translocation in MALT lymphoma, cooperate in a novel NF-κB signaling pathway. J. Biol. Chem. **276**, 19012–19019

7 Rosebeck, S., Rehman, A. O., Lucas, P. C. and McAllister-Lucas, L. M. (2011) From MALT lymphoma to the CBM signalosome: three decades of discovery. Cell Cycle **10**, 2485–2496

8 Snipas, S. J., Wildfang, E., Nazif, T., Christensen, L., Boatright, K. M., Bogyo, M., Stennicke, H. R. and Salvesen, G. S. (2004) Characteristics of the caspase-like catalytic domain of human paracaspase. Biol. Chem. **385**, 1093–1098

9 Coornaert, B., Baens, M., Heyninck, K., Bekaert, T., Haegman, M., Staal, J., Sun, L., Chen, Z. J., Marynen, P. and Beyaert, R. (2008) T cell antigen receptor stimulation induces MALT1 paracaspase-mediated cleavage of the NF-κB inhibitor A20. Nat. Immunol. **9**, 263–271

10 Rebeaud, F., Hailfinger, S., Posevitz-Fejfar, A., Tapernoux, M., Moser, R., Rueda, D., Gaide, O., Guzzardi, M., Iancu, E. M., Rufer, N. et al. (2008) The proteolytic activity of the paracaspase MALT1 is key in T cell activation. Nat. Immunol. **9**, 272–281

11 Hailfinger, S., Nogai, H., Pelzer, C., Jaworski, M., Cabalzar, K., Charton, J. E., Guzzardi, M., Decaillet, C., Grau, M., Dorken, B. et al. (2011) Malt1-dependent RelB cleavage promotes canonical NF-κB activation in lymphocytes and lymphoma cell lines. Proc. Natl. Acad. Sci. U.S.A. **108**, 14596–14601

12 Rosebeck, S., Madden, L., Jin, X., Gu, S., Apel, I. J., Appert, A., Hamoudi, R. A., Noels, H., Sagaert, X., Van Loo, P. et al. (2011) Cleavage of NIK by the API2-MALT1 fusion oncoprotein leads to noncanonical NF-κB activation. Science **331**, 468–472

13 Staal, J., Driege, Y., Bekaert, T., Demeyer, A., Muyllaert, D., Van Damme, P., Gevaert, K. and Beyaert, R. (2011) T-cell receptor-induced JNK activation requires proteolytic inactivation of CYLD by MALT1. EMBO J. **30**, 1742–1752

14 Schechter, I. and Berger, M. (1967) On the size of the active site in proteases. Biochem. Biophys. Res. Commun. **27**, 157–162

15 Edelhoch, H. (1967) Spectroscopic determination of tryptophan and tyrosine in proteins. Biochemistry **6**, 1948–1954

16 Drag, M., Mikolajczyk, J., Krishnakumar, I. M., Huang, Z. and Salvesen, G. S. (2008) Activity profiling of human deSUMOylating enzymes (SENPs) with synthetic substrates suggests an unexpected specificity of two newly characterized members of the family. Biochem. J. **409**, 461–469

17 Maly, D. J., Leonetti, F., Backes, B. J., Dauber, D. S., Harris, J. L., Craik, C. S. and Ellman, J. A. (2002) Expedient solid-phase synthesis of fluorogenic protease substrates using the 7-amino-4-carbamoylmethylcoumarin (ACC) fluorophore. J. Org. Chem. **67**, 910–915

18 Stennicke, H. R. and Salvesen, G. S. (1999) Caspases: preparation and characterization. Methods **17**, 313–319

19 Boatright, K. M., Deis, C., Denault, J. B., Sutherlin, D. P. and Salvesen, G. S. (2004) Activation of caspases-8 and -10 by FLIP(L). Biochem. J. **382**, 651–657

20 Boatright, K. M., Renatus, M., Scott, F. L., Sperandio, S., Shin, H., Pedersen, I. M., Ricci, J. E., Edris, W. A., Sutherlin, D. P., Green, D. R. and Salvesen, G. S. (2003) A unified model for apical caspase activation. Mol. Cell **11**, 529–541

21 Schmidt, U. and Darke, P. L. (1997) Dimerization and activation of the herpes simplex virus type 1 protease. J. Biol. Chem. **272**, 7732–7735

22 Pop, C., Oberst, A., Drag, M., Van Raam, B. J., Riedl, S. J., Green, D. R. and Salvesen, G. S. (2011) FLIP(L) induces caspase 8 activity in the absence of interdomain caspase 8 cleavage and alters substrate specificity. Biochem. J. **433**, 447–457

23 Zhang, Y. and Cremer, P. S. (2006) Interactions between macromolecules and ions: the Hofmeister series. Curr. Opin. Chem. Biol. **10**, 658–663

24 O'Donnell, M. A., Perez-Jimenez, E., Oberst, A., Ng, A., Massoumi, R., Xavier, R., Green, D. R. and Ting, A. T. (2011) Caspase 8 inhibits programmed necrosis by processing CYLD. Nat. Cell Biol. **13**, 1437–1442

25 Yu, J. W., Jeffrey, P. D., Ha, J. Y., Yang, X. and Shi, Y. (2011) Crystal structure of the mucosa-associated lymphoid tissue lymphoma translocation 1 (MALT1) paracaspase region. Proc. Natl. Acad. Sci. U.S.A. **108**, 21004–21009

26 Rawlings, N. D., Morton, F. R., Kok, C. Y., Kong, J. and Barrett, A. J. (2008) MEROPS: the peptidase database. Nucleic Acids Res. **36**, D320–D325

27 Chai, J., Wu, Q., Shiozaki, E., Srinivasula, S. M., Alnemri, E. S. and Shi, Y. (2001) Crystal structure of a procaspase-7 zymogen: mechanisms of activation and substrate binding. Cell **107**, 399–407

28 Riedl, S. J., Fuentes-Prior, P., Renatus, M., Kairies, N., Krapp, S., Huber, R., Salvesen, G. S. and Bode, W. (2001) Structural basis for the activation of human procaspase-7. Proc. Natl. Acad. Sci. U.S.A. **98**, 14790–14795

29 Eichinger, A., Beisel, H. G., Jacob, U., Huber, R., Medrano, F. J., Banbula, A., Potempa, J., Travis, J. and Bode, W. (1999) Crystal structure of gingipain R: an Arg-specific bacterial cysteine proteinase with a caspase-like fold. EMBO J. **18**, 5453–5462

30 Mikolajczyk, J., Boatright, K. M., Stennicke, H. R., Nazif, T., Potempa, J., Bogyo, M. and Salvesen, G. S. (2003) Sequential autolytic processing activates the zymogen of Arg-gingipain. J. Biol. Chem. **278**, 10458–10464

31 Qiu, L. and Dhe-Paganon, S. (2011) Oligomeric structure of the MALT1 tandem Ig-like domains. PLoS ONE **6**, e23220

32 Zhou, H., Du, M. Q. and Dixit, V. M. (2005) Constitutive NF-κB activation by the t(11;18)(q21;q21) product in MALT lymphoma is linked to deregulated ubiquitin ligase activity. Cancer Cell **7**, 425–431

33 Lucas, P. C., Kuffa, P., Gu, S., Kohrt, D., Kim, D. S., Siu, K., Jin, X., Swenson, J. and McAllister-Lucas, L. M. (2007) A dual role for the API2 moiety in API2-MALT1-dependent NF-κB activation: heterotypic oligomerization and TRAF2 recruitment. Oncogene **26**, 5643–5654

34 Malinverni, C., Unterreiner, A., Staal, J., Demeyer, A., Galaup, M., Luyten, M., Beyaert, R. and Bornancin, F. (2010) Cleavage by MALT1 induces cytosolic release of A20. Biochem. Biophys. Res. Commun. **400**, 543–547

35 Riedl, S. J. and Salvesen, G. S. (2007) The apoptosome: signalling platform of cell death. Nat. Rev. Mol. Cell Biol. **8**, 405–413

36 Thornberry, N. A., Rano, T. A., Peterson, E. P., Rasper, D. M., Timkey, T., Garcia-Calvo, M., Houtzager, V. M., Nordstrom, P. A., Roy, S., Vaillancourt, J. P. et al. (1997) A combinatorial approach defines specificities of members of the caspase family and granzyme B. Functional relationships established for key mediators of apoptosis. J. Biol. Chem. **272**, 17907–17911

37 Thornberry, N. A., Bull, H. G., Calaycay, J. R., Chapman, K. T., Howard, A. D., Kostura, M. J., Miller, D. K., Molineaux, S. M., Weidner, J. R., Aunins, J. et al. (1992) A novel heterodimeric cysteine protease is required for interleukin-1β processing in monocytes. Nature **356**, 768–774

38 Stennicke, H. R., Renatus, M., Meldal, M. and Salvesen, G. S. (2000) Internally quenched fluorescent peptide substrates disclose the subsite preferences of human caspases 1, 3, 6, 7 and 8. Biochem. J. **350**, 563–568

39 Drag, M. and Salvesen, G. S. (2010) Emerging principles in protease-based drug discovery. Nat. Rev. Drug Discovery **9**, 690–701

Received 4 January 2012/3 February 2012; accepted 6 February 2012
Published as BJ Immediate Publication 6 February 2012, doi:10.1042/BJ20120035